


Apparent horizon as a membrane

Daniel R. Terno 

School of Mathematical and Physical Sciences, Macquarie University, NSW 2109, Australia

The requirement that a trapped spacetime domain forms in finite time for distant observers is logically possible and sometimes unavoidable, but its consequences are not yet fully understood. In spherical symmetry, the characterization of the near-horizon geometry of these physical black holes is complete and shows marked differences from their eternal counterparts. Whether these differences lead to observable signatures remains unclear. We construct an approximate near-horizon metric that encapsulates them and is suitable for modeling. The timelike apparent horizon of physical black holes provides a natural surface for a consistent membrane description: we obtain closed-form expressions for the redshift, proper acceleration, and extrinsic curvature, and assign a two-dimensional viscous-fluid stress tensor via junction conditions. These results also provide an additional perspective on the relation between Rindler and near-horizon geometries. Among dynamical generalizations of surface gravity, only a subset applies to these models. We complete their analysis and recover the intuitive definition of surface gravity — the acceleration in the frame of a near-horizon observer, redshifted to infinity — directly from the membrane acceleration.

I. INTRODUCTION

More than a hundred astrophysical black holes — dark, massive, ultra-compact objects — have been identified [1, 2]. While all the observations so far are consistent with the classical Kerr solution to Einstein–Hilbert gravity, there are more than a dozen classes of models that purport to provide a detailed description of the observed objects [3, 4]. Their proliferation is possible because the defining textbook feature of a black hole — the event horizon [5–7] — is a teleological concept and is, in principle, inaccessible to local observers [8, 9].

In classical general relativity, *mathematical* black holes (MBHs) — spacetime domains whose interior is causally disconnected from the exterior by a null event horizon — arise only as the asymptotic end state of gravitational collapse. Accepting their formation in finite time entails serious mathematical difficulties and potential paradoxes [6, 9–12].

In contrast with an MBH, a *physical* black hole [13] (Φ BH)¹ is a light-trapping spacetime domain. A locally defined apparent horizon, which is its boundary, is what is actually determined in numerical simulations, particularly in dynamical scenarios [14]. In general, it depends on the foliation of spacetime, which is observer-dependent. We additionally require it to form within a finite time as measured by a distant observer [10, 15].

From the perspective of a distant observer, collapse beyond the Buchdahl [16, 17] limit can proceed in one of three ways: (i) perpetual ongoing collapse, where a horizon exists only as an asymptotic ($t \rightarrow \infty$) concept and, for any $t < \infty$, the nearly frozen configuration remains horizonless by definition; (ii) formation of a horizonless ultra-compact object, either at some finite time t_{\min} or asymptotically as $t \rightarrow \infty$; (iii) formation of an apparent horizon in finite time $t_f < \infty$, as measured by the clock of a distant observer.

Of the three, (i) and (iii) lead to black holes in different senses: (i) approaches an MBH asymptotically ($t \rightarrow \infty$), whereas (iii) yields a black hole in finite time. The Kerr and Schwarzschild MBHs are the asymptotic limit of (i). If we are interested in black holes whose key features have formed by now and are, in principle, observable, we have to select (iii).

At present, most efforts to identify the true nature of astrophysical black holes (ABHs) focus on comparing the models of the first two scenarios [3, 4, 18]. Event horizons are not directly observable, but all current ABH data are consistent with models that explicitly include them. Consequently, viable horizonless proposals have only small, model-dependent deviations that upcoming searches may detect or exclude.

Introducing Φ BHs raises two questions. First, do MBHs and Φ BHs differ in geometric or physical properties? Second, if so, do those differences yield distinct predictions for distant local observers? The first is answered in the affirmative [10], and there are suggestive indications supporting the second [19]. The main goal of this work is to develop an observation-facing framework that translates these differences into testable signatures.

The requirements of finite t_f and minimal regularity conditions of the apparent horizon allow, in spherical symmetry, a complete classification of the near-horizon geometries. Some of their properties are conceptually different from both the Schwarzschild solution and regular black hole models. In Section II, after reviewing our self-consistent framework and the essential properties of the Φ BH solutions, we discuss how the dynamical solutions can describe astrophysically relevant nearly static configurations.

The apparent horizon of a Φ BH is a timelike surface. This makes it natural to apply the membrane (or stretched-horizon) formalism. We do so in Section III, where we also discuss additional aspects of the relationship between the near-horizon geometry of a Φ BH and the Rindler geometry. The membrane viewpoint completes the analysis of various generalisations of surface gravity to dynamical spacetimes, which we report in Section IV. We conclude with the discussion and an outline of future work in Section V.

Throughout this article, we work in natural units $G = c = \hbar = 1$. The outer apparent horizon is at the Schwarzschild

* daniel.terno@mq.edu.au

¹ The term “physical black hole” was introduced in Ref. [13] and is abbreviated as PBH in Ref. [10] and elsewhere. Because PBH is also the standard acronym for “primordial black hole,” we adopt a distinct abbreviation here to avoid confusion.

radius $r_g(t) = r_+(v)$, that we express using the time coordinate t and the advanced null coordinate v , respectively. When convenient, the coordinate distance from the Schwarzschild radius is denoted $x := r - r_g$ or $y := r - r_+$, depending on the coordinates used. A prime denotes differentiation: $r'_+ := dr_+/dv$ and $r'_g := dr_g/dt$. To shorten descriptions, we refer to a distant static observer as Bob, a horizon-crossing observer as Alice, and a static or comoving observer as Eve. We use fractional subscripts only for small fractions and omit the fraction bar, so $h_{1/2}$ is written as h_{12} .

II. PROPERTIES OF PHYSICAL BLACK HOLES

A. The framework

The very posing of the collapse trilemma assumes the classical geometric picture inherent to semiclassical gravity. The phenomena such as generation of gravitational waves and their propagation, motion of test particles, or light propagation are assumed to occur as in general relativity or some alternative classical theory of gravity. The semiclassical description incorporates quantum expectation values for the renormalised energy-momentum tensor (EMT) of matter fields into the classical framework. In this setting, the metric $g_{\mu\nu}$ is a solution to the semiclassical Einstein equations [11, 20–22]

$$R_{\mu\nu} - \frac{1}{2}g_{\mu\nu}R = 8\pi T_{\mu\nu}, \quad (1)$$

where $R_{\mu\nu}$ and R are the Ricci tensor and scalar, and the right hand side is the effective EMT. It includes the renormalized expectation value of all matter fields, higher-order terms arising from its regularisation, and possible contributions arising from modifications to Einstein-Hilbert gravity or a cosmological constant Λ . However, our analysis does not use any specific property of the quantum state of matter and does not separate the matter EMT into the collapsing matter and (perturbatively-obtained) quantum excitations [10].

In discussing Φ BH properties we apply the weakest form of cosmic censorship and require the absence of scalar curvature singularities at the apparent horizon [5, 6]. In spherical symmetry it is enough to require that $G^\mu_\mu =: \mathbb{G}$ and $G_{\mu\nu}G^{\mu\nu} =: \mathbb{G}$ are finite [10]. We express this observability by requiring a finite formation time according to the clock of a distant Bob.

A general spherically symmetric metric in Schwarzschild coordinates (with areal radius r) is given by

$$ds^2 = -e^{2h(t,r)}f(t,r)dt^2 + f(t,r)^{-1}dr^2 + r^2d\Omega_2, \quad (2)$$

while using the advanced null coordinate v results in the form

$$ds^2 = -e^{2h_+(v,r)}f_+(v,r)dv^2 + 2e^{h_+(v,r)}dvdr + r^2d\Omega_2. \quad (3)$$

The function f is coordinate-independent, i.e. $f(t,r) \equiv f_+(v(t,r),r)$ and in what follows we omit the subscript. It is conveniently represented via the Misner–Sharp–Hernandez

(MSH) mass $M_M \equiv C/2$ [7] as

$$f = 1 - \frac{C(t,r)}{r} = 1 - \frac{C_+(v,r)}{r} := \partial_\mu r \partial^\mu r, \quad (4)$$

The functions h and h_+ play the role of integrating factors in the coordinate transformation

$$dt = e^{-h}(e^{h_+}dv - f^{-1}dr). \quad (5)$$

For example, the Schwarzschild metric corresponds to $h \equiv 0$, $C_M \equiv r_g = \text{const}$, and $v = t + r_*$, where r_* is the tortoise coordinate [5, 6].

In a cosmological setting we assume that a separation of scales exists between geometric features associated with the black hole and those of the large-scale universe [19, 23]. In this case, the outer apparent horizons of the Φ BH is given by the largest real root r_g of $f(t,r) = 0$ that is belongs to the near-region, i.e. $r_g \ll 1/\sqrt{\Lambda}$. Invariance of the MSH mass implies

$$r_g(t) = r_+(v(t, r_g(t))), \quad (6)$$

where r_+ is the equivalent root of $f(v,r)$. Unlike the globally defined event horizon, the apparent horizon is foliation-dependent. However, it is invariantly defined in all foliations that respect spherical symmetry [24] which will be used in the following.

Both the analysis of the Einstein equations and the evaluation of curvature invariants are conveniently performed using the effective EMT components τ_a , (where $a = t, r, t^r$) defined as [10]

$$\tau_t := e^{-2h}T_{tt}, \quad \tau^r := T^{rr}, \quad \tau_t^r := e^{-h}T_t^r. \quad (7)$$

The Einstein equations for the components G_{tt} , G_t^r , and G^{rr} are then, respectively

$$\partial_r C = 8\pi r^2 \tau_t / f, \quad (8)$$

$$\partial_t C = 8\pi r^2 e^h \tau_t^r, \quad (9)$$

$$\partial_r h = 4\pi r (\tau_t + \tau^r) / f^2. \quad (10)$$

To ensure finite values of the curvature scalars, it is sufficient to work with only two invariant quantities

$$\mathbb{G} = \mathbb{T} + 2T_\theta^\theta, \quad \mathbb{G} := \mathbb{T} + 2(T_\theta^\theta)^2, \quad (11)$$

where

$$\mathbb{T} = (\tau^r - \tau_t) / f, \quad (12)$$

$$\mathbb{T} = ((\tau^r)^2 + (\tau_t)^2 - 2(\tau_t^r)^2) / f^2. \quad (13)$$

In our analysis we can disregard the contributions of $T_\theta^\theta \equiv T_\phi^\phi$, as one can verify that they do not introduce further divergences [10, 25].

B. Solutions

There are two admissible classes of near-horizon solutions which are distinguished by the behaviour of the effective EMT components as $r \rightarrow r_g$, which scale as f^k with $k = 0, 1$ [10, 25]. Solutions with $k = 1$ describe eternal static configurations and the moments of formation and possible evaporation of a Φ BH [10, 23]. Dynamics of a Φ BH through its evolution is described by a $k = 0$ solution, where the three effective EMT components scale as

$$\tau_t, \tau^r \rightarrow -\Upsilon^2, \quad \tau_t^r \rightarrow \pm\Upsilon^2, \quad (14)$$

for some $\Upsilon(t)$. The two metric functions are

$$C = r_g - 4\sqrt{\pi}r_g^{3/2}\Upsilon\sqrt{x} + c_1x + \mathcal{O}(x^{3/2}), \quad (15)$$

$$h = -\frac{1}{2}\ln\frac{x}{\xi} + h_{12}\sqrt{x} + \mathcal{O}(x), \quad (16)$$

where $x := r - r_g(t)$, and the function $\xi(t)$ is determined by the choice of time variable. As a result,

$$f = \alpha_{12}\sqrt{x} + \mathcal{O}(x), \quad \alpha_{12} = 4\sqrt{\pi}r_g\Upsilon. \quad (17)$$

The higher order terms such as $c_1(t)$ and $h_{12}(t)$ are discussed in Appendix A 1

As only two metric functions — $f(t, r)$ and $h(t, r)$ — describe solutions of the Einstein equations, consistency of Eq. (9) with Eqs. (8) and (10) requires that

$$\frac{dr_g}{dt} \equiv r'_g = \pm 4\Upsilon\sqrt{\pi r_g \xi} = \pm \alpha_{12}\sqrt{\xi}, \quad (18)$$

where the plus (minus) sign corresponds to the expansion (contraction) of the outer horizon. The case of $r'_g < 0$ is most conveniently described using the advanced null coordinate v . An evaluation of the expansions of null geodesic congruences [5, 7] identifies the domain $f < 0$ as a trapped region, and thus a Φ BH. The case of $r'_g > 0$ is most conveniently described using the retarded null coordinate u . In this case the domain $f < 0$ is the anti-trapped region. Here we are concerned only with black holes.

The function $-\Upsilon^2 < 0$ determines the energy density at the outer apparent (or anti-trapping) horizon, and higher-order terms are matched with higher-order terms in the EMT expansion [10]. Both solutions violate the null energy condition (NEC) in the vicinity of the horizon at $r = r_g$ [5, 26], i.e. there are future-directed null vectors k^μ such that $T_{\mu\nu}k^\mu k^\nu < 0$. This is consistent with the result that the apparent horizon is not ‘visible’ to a distant observer unless the NEC is violated [5, 6].

In (v, r) coordinates the black hole metric is described by

$$C_+(v, r) = r_+(v) + w_1(v)y + \mathcal{O}(y^2), \quad (19)$$

$$h_+(v, r) = \zeta_0(v) + \zeta_1(v)y + \mathcal{O}(y^2), \quad (20)$$

where $y := r - r_+(v)$. Note that a freedom in the redefinition of the null variable v allows one to set $\zeta_0 \equiv 0$. From the definition of the apparent horizon it follows that $w_1 \leq 1$.

The inequality is saturated at the formation of a Φ BH (more details can be found in [27]). We discuss relations between the expressions of the metric functions in the two coordinate systems and behaviour of some of the expansion coefficients below.

The Schwarzschild sphere $r_g(t)$ is a timelike hypersurface [10?]. Therefore, ingoing null geodesics and some of the ingoing timelike geodesics cross the apparent horizon in a finite time according to Bob. This property also is the basis for its use as a natural redshift regulator in the membrane paradigm in Section III.

The ingoing null geodesics satisfy

$$\left. \frac{dr}{dt} \right|_{v=\text{const}} = -e^h f = r'_g - \ell_{12}\sqrt{x} - \frac{\ell_1}{r_g}x + \mathcal{O}(x^{3/2}). \quad (21)$$

Here the coefficient ℓ_{12} is expressed via the redshift at the apparent horizon, $d\tau^2 = \alpha^2 dt^2|_H$, as

$$\ell_{12} = \frac{\alpha^2}{2\sqrt{\xi}}, \quad (22)$$

and the coefficient ℓ_1 will be discussed below. The redshift for a comoving observer at the apparent horizon, $r_g(t) \equiv r_H(\tau)$ and is given by

$$\begin{aligned} \alpha^2 &= \lim_{r \rightarrow r_g} (e^{2h} f^2 - r_g'^2) / f \\ &= \frac{2\xi}{r_g} (1 - c_1 + 4\sqrt{\pi}h_{12}r_g^{3/2}\Upsilon) \end{aligned} \quad (23)$$

Using invariance of the MSH mass and Eq. (5) it is possible to obtain relations between the coefficients of the metric function expansions in the two coordinate systems. For example, the leading order relation between the coordinate distances from the horizon, $x(t(v, r), r)$ and y is by

$$x = \frac{1}{2}\omega^2 y^2, \quad \omega^2 = \frac{\alpha^4}{8\xi r_g'^2} \quad (24)$$

Appendix A 2 provides the details of the derivations of this and related relations.

There are several useful relations that hold on the apparent horizon. Coordinate-independent definition of the MSH mass and the timelike character of apparent horizon result in

$$\left. \frac{dv}{dt} \right|_H = \frac{|r'_g|}{|r'_+|} = \frac{\alpha}{\sqrt{2|r'_+|}}, \quad (25)$$

respectively. On the other hand, Eq. (5) implies

$$\left. \frac{dv}{dt} \right|_H = \frac{\ell_{12}}{\alpha_{12}}. \quad (26)$$

As we discuss in Section IV the well-defined generalisation of the surface gravity to spherically-symmetric dynamical are approximately (or exactly, Hayward–Kodama surface gravity κ_K) are equal to $(1 - w_1)/(2r_+)$. It coincides with the Schwarzschild value $\kappa = 1/4M = 1/2r_g$ only if $w_1 = 0$.

We will use this value throughout, both because this is the basis for the Hawking temperature [11, 12], and especially because even small deviations of the first mass expansion coefficient from zero have dramatic influence on the QNM spectrum [28].

Hence unless it is assumed otherwise we set $w_1 = 0$, which leads to

$$\alpha^2 = \frac{4\xi}{r_g}. \quad (27)$$

Assuming that $\kappa_K = (2r_g)^{-1}$ and that the Page evaporation law [6, 12, 29] has the same form in both (t, r) and (v, r) coordinates, with $r'_g = -A/r_g^2$, $r'_+ = -A/r_+^2$, respectively, leads to the identification [23]

$$\Upsilon^2 = \frac{A}{8\pi r_g^4}, \quad \xi = \frac{A}{2r_g}. \quad (28)$$

It allows us to identify

$$\alpha^2 = \frac{4\xi}{r_g} = 2|r'_g|, \quad \ell_{12} = \frac{\alpha}{\sqrt{r_g}}. \quad (29)$$

In addition, adapting the arguments of [30] that in a steady state approximation of the black hole evaporation [6, 12] we obtain

$$\zeta_1 \sim |r'_+|/r_+. \quad (30)$$

Hence in the near horizon region $h_+ \approx 0$, and the metric in (v, r) coordinates as well approximated by a Vaidya metric with $2M(v) = r_+(v)$.

C. Static limit

Apart from a strikingly different form of the metric of Eqs. (15) and (16), the differences from MBHs include violation of the NEC and the finite infall time according to a distant observer. Hence it is interesting and important to investigate potential observable consequences that follow from these differences. One technical difficulty is that Eqs (9) and (13) indicate that there are no static $k = 0$ solutions. In fact, all static black hole models indeed belong to the class $k = 1$.

However, outside the dramatic astrophysical events such as collisions [1, 4, 14], ABH are essentially stationary and modelled as such [3, 6, 14, 31]. For macroscopic objects, even is small as primordial black holes [32, 33] with high expected Hawking temperature, the dynamical evolution is slow [34, 35]. Hence we have to put the Φ BH metrics into the form that allows immediate comparison with their static counterparts.

We focus on the limiting form of the near horizon geometry, as this is the domain where the differences between the Φ BHs and MBHs may be observed. From a mathematical point of view the limit is naturally described in (v, r) coordinates, where all metric parameters in Eqs. (A5) and (20) become constant, and $y \rightarrow x$. As majority of the static models

have $h_+ \equiv h = 0$ we will assume this here. The transition to the static limit is conveniently analysis by assuming validity of the Page evaporation law and then taking the limit $A \rightarrow 0$.

Description of the transition in (t, r) coordinates is more involved. The static metric function $f(r)$ belongs to $k = 1$ class and has the near horizon expansion [28]

$$f(r) = \sum_{k \geq 1} \frac{\bar{\alpha}_k}{r_g^k} x^k. \quad (31)$$

We are interested in a sufficiently smooth transition

$$f(t, r) = \sum_{k \in \mathbb{Z}/2} \frac{\alpha_k}{r_g^k} x^k \rightarrow f(x), \quad (32)$$

while $|r'_g| \rightarrow 0$. That means in the expansion of $g^{rr} \equiv f = 1 - C(t, r)/r$ all coefficients of the half-integer powers $x^{(2j+1)/2}$ approach zero, and the coefficients of the integer powers approach the static values, e.g.,

$$\alpha_1 = 1 - c_1 \rightarrow \bar{\alpha}_1, \quad \alpha_2 = -1 + c_1 - c_2 r_g \rightarrow \bar{\alpha}_2. \quad (33)$$

Indeed, $r'_g \rightarrow 0$ and additional relations of the previous Section imply that $\Upsilon \rightarrow 0, \xi \rightarrow 0$ individually, while the appropriate behaviour of the higher order EMT components ensures a smooth approach to the static limit.

On the other hand, using Eq. (16) to write

$$e^h = \sqrt{\frac{\xi}{x}} \exp\left(\sum_{j \geq 1} h_{j/2} x^{j/2}\right) =: \sqrt{\frac{\xi}{x}} e^{\bar{h}}, \quad (34)$$

clearly shows that the static limit of the series expansion that necessarily involves $\xi \rightarrow 0$ is singular, with the coefficients in the expansion of \bar{h} diverging as powers of $1/\xi$. Hence we demand only that in the asymptotically flat case $e^h \rightarrow 1$, so

$$e^{h(t,r)} f(t, r) \rightarrow f(r), \quad e^{2h(t,r)} f(t, r) \rightarrow f(r), \quad (35)$$

and use the approximations that satisfy this limit and give the correct form of a sufficient number of the expansion coefficients $h_{j/2}$ at finite r'_g . We discuss the approximate form of e^h in Appendix A 3

The coordinate transformation of Eq. (5) becomes the standard transformation for the Eddington-Finkelstein coordinates, $dv = dt + dr/f$. The first two terms in the expansion $e^h f$ of Eq. (21) go to zero as $r'_g \rightarrow 0$ (again, conveniently modelled by $A \rightarrow 0$), and $e^h \rightarrow 1$ means $\ell_1 \rightarrow \alpha_1$.

It is also straightforward to see that only the leading half-integer order terms are of consequence for any $A < 1$. For nonzero r'_g it is also possible to study motion of the test particles or response to gravitational perturbations by ‘‘freezing’’ the metric, as the characteristic time scales of these processes are much shorter than the Φ BH characteristic time $r_g/|r'_g| \sim r_g^3/A$. Indeed, taking $\alpha_1 \sim 1$ we get the estimate of the range of the coordinate distance from the apparent horizon where the deviations of the frozen metric that approximates the Φ BH geometry via Eq. (37) from the static metric of Eq. (31) by identifying x_* for which the first two terms of

Eq. (37) coincide,

$$\frac{x_*}{r_g} = \alpha^2 \sim |r'_g|. \quad (36)$$

For the same value $x = x_*$ the contribution of the next term $\alpha_{3/2}x^{3/2}/r_g^{3/2}$ is smaller by the factor of α .

Travel time up x_* is well approximated by the standard classical result. Eq. (21) then indicates that the time that it takes to complete the infall is $\Delta t_* = \mathcal{O}(r_g)$. Thus the natural Φ BH cut-off on a blueshift $1/\alpha$ ensures that the actual infall takes of the order of the black-hole light-crossing time r_g .

As a result, the simplest explicit form of the Φ BH-modified metric functions that satisfy all these requirements are given by

$$f = \alpha_{12}\sqrt{x} + \frac{\alpha_1}{r_g}x + \mathcal{O}(x^2), \quad (37)$$

$$e^h = \sqrt{b^2 + \frac{\xi}{x}} + d, \quad (38)$$

where $\alpha_{12} = 4\sqrt{\pi r_g \Upsilon}$, and $b + d = 1$ (or another asymptotic value), and $h_{12} = d/\sqrt{\xi}$.

III. APPARENT HORIZONS AS MEMBRANES

Φ BHs provide a natural regulator for the redshift and the free-fall acceleration in the frame of the observer at the horizon. This suggests treating their apparent horizons as membranes [36], and below we derive some of their basic properties. Relationships between the near-horizon geometry of a black hole and the Rindler geometry are profound, intriguing, and potentially important. They can be put on a rigorous basis for Φ BHs if a particular hypersurface, known as the York–Frolov separatrix, is used as a baseline [46]. In Section III B we show that it is also a hypersurface of approximately zero redshift.

A. Basic membrane properties

In classical general relativity, freely falling observers should experience no special event as they cross the event horizon of an MBH. However, to a distant static observer (Bob) an infalling observer (Alice) appears to be frozen at the horizon due to the infinite redshift effect. Hence, the BH interior can be regarded as irrelevant for a distant observer. The membrane paradigm [36] is based on this complementary picture. Accordingly, a distant observer excludes the interior of an MBH by a fictitious timelike membrane (also known as a stretched horizon), located at some coordinate distance ϵ outside the horizon.

The two most basic quantities that are needed to characterise this surface at some $r = r_g + \epsilon$, $\epsilon \ll r_g$ [36] are the redshift and the free fall acceleration that is experienced by a static observer (Eve) there. For a hairless static MBH of

Section II C, these are

$$\alpha = \sqrt{f(r)}, \quad g = \frac{f'(r)}{2\sqrt{f}} \rightarrow \frac{\kappa}{\alpha}, \quad (39)$$

respectively, where κ is the surface gravity. We discuss different dynamical generalisations of the surface gravity in Section IV.

Using the Israel junction conditions [37] the membrane is endowed with the EMT of a 2D viscous fluid whose physical properties are such that the membrane has the same phenomenology of the BH [36, 38–40]. A careful analysis of membrane's properties led to Ohm's law, Joule's law, and the non-relativistic Navier–Stokes equation.

In a fully classical picture there is a peculiar relations between the shear viscosity η and the bulk viscosity ζ ,

$$\eta_{\text{MBH}} = -\zeta_{\text{MBH}} = \frac{1}{16\pi}. \quad (40)$$

In general, viscosity depends on quantum corrections. In membrane's role as a boundary condition proxy viscosity affects reflectivity [38–40],

$$|\mathcal{R}| = \left| \frac{1 - \eta/\eta_{\text{MBH}}}{1 + \eta/\eta_{\text{MBH}}} \right|, \quad (41)$$

and is thus directly tied to the boundary conditions that are imposed in black hole perturbation problems.

The Φ BH framework provides a natural candidate for the membrane – the contracting timelike apparent horizon. As the (v, r) coordinates are regular across the horizon we mostly use them for the analysis below, but physically relevant quantities can be extracted also using the Schwarzschild coordinates.

The results of Section II B indicate that the redshift $\alpha \sim \sqrt{2|r'_g|}$. Intruding α_v via $d\tau^2 = \alpha_v^2 dv^2|_{\text{H}}$, we have

$$\alpha_v^2 = 2|r'_+(v)|. \quad (42)$$

The apparent horizon is a timelike hypersurface given by an implicit equation $\Phi = r - r_+(v) = 0$. Its spacelike unit normal $n_\mu \propto \partial_\mu \Phi$. The four-acceleration $a^\mu = Du^\mu/d\tau$ is proportional to it,

$$a^\mu = g_v n^\mu, \quad n_\mu = -\frac{1}{\sqrt{2}} \left(\sqrt{|r'_+|}, 1/\sqrt{|r'_+|}, 0, 0 \right). \quad (43)$$

Its magnitude is

$$g_v = -\frac{(1 - w_1)r'_+ + 2\zeta_1 r_+ r'^2_+ + r_+ r''_+}{2\sqrt{2}r_+ |r'_+|^{3/2}}, \quad (44)$$

which on the approach to the static limit (Section II C) becomes

$$g_v \rightarrow \left(2\sqrt{2|r'_+|} r_+ \right)^{-1}. \quad (45)$$

The apparent horizon is coordinatised by the proper time τ and the angular variables θ and ϕ . The triad on the apparent

horizon e_a^μ , $a = 0, 2, 3$ is formed by the four-velocity u^μ of a comoving observer and the two tangent vectors ∂_θ and ∂_ϕ , respectively. We comment in passing that in the original spirit of the membrane paradigm the acceleration of a freely-falling Alice in the reference frame of the comoving Eve on the apparent horizon is $-g_v$, directed “downwards”.

The extrinsic curvature $K_{ab} = n_{(\mu;\nu)}e_a^\mu e_b^\nu$ has diagonal form,

$$K_b^a = \text{diagonal} \left(g_v, \frac{\alpha_v}{2r_+}, \frac{\alpha_v}{2r_+} \right), \quad (46)$$

where the dependence on $v = v(\tau)$ is assumed. We contrast it with the extrinsic curvature tensor in a static spherically symmetric gravitational field with $h \equiv 0$,

$$K_b^a = \text{diagonal} \left(g, \frac{\alpha}{r}, \frac{\alpha}{r} \right), \quad (47)$$

which is evaluated for a surface at $r = \text{const}$.

A fictitious matter distribution on the membrane is obtained by formally postulating discontinuity in transversal metric components between the two bulk regions, outside (\mathcal{M}^+) and inside (\mathcal{M}^-) of the membrane. Following [36] we set $K_{ab}^+ := K_{ab}$, $K_{ab}^- \equiv 0$ (an alternative convention [38, 41] is $K_{ab}^- = -K_{ab}^+$). The hypersurface EMT S_b^a is introduced via the Israel junction condition [37],

$$[K]\delta_b^a - [K_b^a] = 8\pi T_b^a, \quad (48)$$

where $[\]$ indicates that the difference between the outside and the inside values of the relevant quantity is taken at the membrane. In a general case it has the form corresponding to a two-dimensional dissipative fluid [36, 38],

$$T_{ab} = \rho u_a u_b + (p - \zeta \vartheta) \gamma_{ab} - 2\eta \sigma_{ab}. \quad (49)$$

The projector tensor $\gamma_{ab} := h_{ab} + u_a u_b$ is defined using the induced metric $h_{ab} := g_{\mu\nu} e_a^\mu e_b^\nu$ on the membrane. For the h_{ab} -metric compatible covariant derivative D_a the expansion and the shear are defined as $\vartheta = D_a u^a$ and $\sigma_{ab} := \frac{1}{2}(\gamma_b^c D_c u_a + \gamma_a^c D_c u_b - \vartheta \gamma_{ab})$. In contrast to the static background (where both the shear and the expansion are zero), here

$$\vartheta = \frac{2\dot{r}_+(\tau)}{r_+(\tau)} = -\frac{\alpha_v}{r_+}, \quad \sigma_{ab} = -\frac{\vartheta}{2} \gamma_{ab}. \quad (50)$$

If one still accepts $\eta = -\zeta = 1/(16\pi)$, then the two-dimensional density and pressure are

$$\rho = -\frac{\alpha_v}{8\pi r_+}, \quad (51)$$

$$p = \frac{1}{8\pi} \left(g_v + \frac{3}{2} \frac{\alpha_v}{r_+} \right) \approx \frac{1}{6\pi r_+} \left(\frac{1}{\alpha_v} + 3\alpha_v \right). \quad (52)$$

Analogously to the standard membranes, in the static limit $r'_g \rightarrow 0$ energy surface density goes to zero while the two-dimensional pressure diverges with g_v .

We can formally define the speed of sound on the membrane $c_s = \sqrt{\partial p / \partial \rho}$, [39, 42]. To express the isentropic

condition [14] we treat both quantities as functions of α_v (i. e. the evaporation rate), and keep the Schwarzschild radius constant. Then

$$c_s \approx \frac{1}{2\alpha_v^2} \gg 1, \quad (53)$$

diverging in the static MBH limit, also similarly to the standard membrane case.

B. Separatrix

An elegant mathematical relation between the near horizon Schwarzschild (or Kerr) metric and the Rindler metric [11, 12] is useful for the analysis of the Hawking radiation and serves as a starting point of many aspects of gravitational thermodynamics [12, 43–45]. In the Schwarzschild case near the event horizon the two-dimensional part of metric is

$$ds^2 \approx -\frac{x}{r_g} dt^2 + \frac{r_g}{x} dx^2 = -\kappa^2 \mathfrak{x}^2 dt^2 + d\mathfrak{x}^2 + dL_\perp^2, \quad (54)$$

where a new independent variable \mathfrak{x} corresponds to the physical distance from the horizon,

$$\mathfrak{x} = \int_{r_g}^{r_g+x} \frac{dr}{\sqrt{f(r)}}, \quad (55)$$

and κ is the surface gravity. The association of κ as acceleration and (t, \mathfrak{x}) as the Rindler coordinates allows the standard conformal mapping into the two-dimensional Minkowski spacetime.

Despite importance of the Rindler–Schwarzschild relation, its rigorous establishment is non entirely straightforward. Expansion near the apparent horizon of a Φ BH does not lead to anything resembling the right hand side of Eq. (54). The key insight of Ref. [46] was to take a special hypersurface — the York–Frolov separatrix [47–49] as the base.

It was originally introduced [47] to provide an approximate locally-derived expression for the event horizon. If it forms, the event horizon is a null surface that is generated by the last family of outgoing null geodesics $R(v)$ that do not reach future null infinity. For a future-directed outgoing family of null geodesics, one of which family we denote $R(v)$, at the apparent horizon of a Φ BH both expansion $\vartheta_{\text{out}} = 0$ and $R'(v) = 0$ are zero. The photons are only momentarily at rest and escape to finite distances in finite (advanced) time. On the other hand, the event horizon generators are photons that are “stuck”, which can be quantified as $d^2 R / dv^2 = 0$. Thus the solution $r_{\text{sep}}(v)$ of the algebraic equation

$$2 \frac{d}{dv} (e^h f) + e^h f \frac{d}{dr} (e^h f) = 0, \quad (56)$$

provides a good approximation for the location of the event horizon.

For low luminosity $L \ll 1$, a perturbative analysis establishes that $r_{\text{sep}}(v)$ is close to r_+ . Thus we obtain the leading-order expression for $y_{\text{sep}} := r_{\text{sep}}(v) - r_+(v)$ for a sufficiently

small w_1 is given by

$$y_{\text{sep}} \cong 2r_+(1 + w_1)r'_+. \quad (57)$$

while a more general expression is given in Appendix B.

Event horizons are absent in regular black holes. In many of their models it is still a useful distinction between null and timelike geodesics that can leave the trapped region only at its final disappearance and those that can cross the timelike apparent horizon before the evaporation is complete. The boundary of the two domains is a null geodesic (named a D-geodesic [49]). The condition of Eq. (56) is much easier to implement, and the resulting separatrix $r_{\text{sep}}(v)$ is a good approximation to it.

The separatrix plays a role similar to the event horizon also in its another aspect. In a static ($k = 1$) case the redshift of a static Eve approaches zero according to Eq. (39) when her position approaches the event horizon. For slow evolving Φ BH wit $\zeta \sim |r'_+|/r$ and $w_1 \ll 1$ for an observer at $r_{\text{sep}}(v)$ that moves with the same (coordinate) velocity as the comoving horizon observer, $dr/dv = r_+$, the redshift is approximately zero. Indeed, using Eq. (3) we find

$$d\tau^2 = \mathcal{O}(w_1^2|r'_+|, |r'_+|^2)dv^2. \quad (58)$$

IV. SURFACE GRAVITY

The surface gravity κ plays an important role in particularly in black hole thermodynamics and more generally in semi-classical gravity [5, 11, 12, 50]. For an observer at infinity the Hawking radiation that is produced on the background of a stationary black hole is thermal with its temperature given by $\kappa/2\pi$. However, surface gravity is unambiguously defined only in stationary spacetimes, where there are several equivalent definitions.

Stationary asymptotically flat spacetimes admit a Killing vector field ξ^μ , $\xi^\mu \xi_{(\mu;\nu)} = 0$, that is timelike at infinity [5, 7]. A Killing horizon is a hypersurface on which the norm $\sqrt{\xi^\mu \xi_\mu} = 0$. While logically this concept is independent of the notion of an event horizon, the two are related: in a stationary asymptotically flat spacetime the event horizon coincides with the Killing horizon [6]. The Killing property $\xi_{(\mu;\nu)} = 0$ results in $\xi^\mu \xi_\mu = \text{const}$ on each of its integral curves, and the surface gravity κ can be introduced as the inaffinity of null Killing geodesics on the event horizon,

$$\xi^\mu_{;\nu} \xi^\nu := \kappa \xi^\mu. \quad (59)$$

On the other hand, assuming sufficient regularity of the metric, expansion of the null geodesics near the apparent horizon $r > r_g$ then establishes the concept of peeling affine gravity [51, 52],

$$\frac{dr}{dt} = \pm 2\kappa_{\text{peel}}(t)x + \mathcal{O}(x^2). \quad (60)$$

Finally, κ can be intuitively described as the force that would be required by an observer at infinity to hold a parti-

cle (of unit mass) stationary at the event horizon. For a static observer Eve at some fixed areal radius r the square of her four-acceleration g_E^2 satisfies

$$g_E(r) := \sqrt{a_E^\mu a_{E\mu}} = \frac{r_g}{2r^2 \alpha_E}, \quad (61)$$

where the redshift $\alpha_E \equiv \sqrt{|g_{00}|} = e^h \sqrt{f} = \sqrt{1 - r_g/r}$. Correcting for it and taking Eve's position to the horizon results in the surface gravity,

$$\kappa = \lim_{r \rightarrow r_g} \alpha_E g_E = \frac{1}{2} f'(r_g) = 1/(2r_g). \quad (62)$$

(where for a general static metric the redefinition of time allows to set $h(r_g) = 0$, and the last equality is valid for the Schwarzschild metric).

Generalisations of these definitions to general spacetimes are inequivalent, but for slowly evolving macroscopic black holes are thought to give close results [51, 53]. In spherically-symmetric spacetimes Kodama vector field [54] has many properties of the Killing field and results in the expression for surface gravity [7, 55]

$$\kappa_K = \frac{1}{2} \left(\frac{C_+}{r^2} - \frac{\partial_r C_+}{r} \right) \Big|_{r=r_+} = \frac{(1 - w_1)}{2r_+}. \quad (63)$$

It is well-defined for Φ BHs and if one requires that its value corresponds to the standard surface gravity (which is necessary for the validity of the black hole evaporation seen as a sequence of the Schwarzschild background snapshots [6, 12]), then $w_1 = 0$ must hold.

A naive application of Eq. (62) leads to a divergent quantity [10], seemingly invalidating the relationship between the surface gravity and acceleration at the horizon. Below we show how it can be correctly extended to dynamical spacetimes.

There are several versions of the peeling surface gravity that run into difficulty because their definitions presuppose at least continuity of the function $h(t, r)$ on the apparent horizon. The only definition that does not trivially result in zero or infinity [56] was introduced using flat slice Painlevé–Gullstrand coordinates (\bar{t}, r) [53] (whose relevant properties are summarized in Appendix C),

$$\kappa_{\text{PG}_2} := \frac{1}{2r_g} (1 - \partial_r \bar{C} + \partial_{\bar{t}} \bar{C}) \Big|_{r=r_g}, \quad (64)$$

where $\bar{C}(\bar{t}, r) = 2M(t(\bar{t}, r), r)$ is the MSH mass expressed in the Painlevé–Gullstrand (PG) coordinates. It was shown [56] that

$$\kappa_{\text{PG}_2} = \frac{\partial_{\bar{t}} \bar{C}}{2r_g} \Big|_{r=r_g}, \quad (65)$$

where

$$\partial_{\bar{t}} \bar{C} = \partial_{\bar{t}} C \partial_{\bar{t}} t|_r. \quad (66)$$

Thus

$$\partial_t \bar{C} \approx \frac{r'_g}{\partial_t \bar{t}} \left(1 + \frac{2\sqrt{\pi r_g^3 \Upsilon}}{\sqrt{r - r_g}} \right), \quad (67)$$

and the behavior of the function $\bar{t}(t, r)$ near the apparent horizon determines the limit. As we found that $\partial_t \bar{t} \approx 1$ in its vicinity (see Appendix C), this version of the surface gravity is also untenable for a Φ BH.

On the other hand, if we modify the intuitive description of κ by replacing the static observer Eve with the one comoving with the contracting apparent horizon, for a slowly evolving Φ BH

$$\lim_{r \rightarrow r_+} \alpha_v g_v \approx \frac{1 - w_1}{2r_+} \rightarrow \kappa, \quad (68)$$

where g_v is given by Eq. (45), and the limit corresponds to $w_1 = 0$, which is the exact coincidence condition for the Kodama surface gravity.

V. DISCUSSION

Despite the main $k = 0$ family of solutions not having static metrics, it is possible to study their static limit in which the $k = 1$ MBHs are approached. The resulting frozen $k = 0$ metric of Eqs. (37) and (38) is a suitable starting point for the analysis of the quasinormal modes (QNMs) and light rings of Φ BHs. The near- and far-region geometries can be connected using Pad'e approximants [58–60]. The $\alpha_{12}\sqrt{x}$ term fits the interpolation scheme of Ref. [28], while the approximation to e^h will be used directly.

Independently of the slow-evolution assumption, the first steps in implementing the membrane paradigm and a consistent description of the boundary conditions in terms of a 2D fluid on a timelike apparent horizon are carried out: local redshift, proper acceleration, relevant extrinsic data, and a viscous-fluid EMT are obtained. These data parameterise dissipation/reflectivity and can be used to assess their impact on quasinormal spectra and possible echoes at any rate of dynamics.

For surface gravity, the remaining peeling-type generalisation is ruled out for Φ BHs. On the other hand, the intuitive interpretation of the surface gravity in stationary spacetimes — proper acceleration of an observer just outside the horizon, redshifted to infinity — is naturally extended to dynamical Φ BHs. It is close to the well-defined Kodama–Hayward surface gravity. The latter coincides with the momentarily Schwarzschild value $\kappa = 1/(4M)$ only when the expansion parameter $w_1 = 0$.

Our results provide lay the necessary background for the quantitative evaluation of the light rings, QNMs and possible echo structures for Φ BHs and their comparison with the standard results in spherical symmetry. This will be the subject of the subsequent works.

ACKNOWLEDGMENTS

This work was supported by the ARC Discovery project Grant No. DP210101279 and by the Schwinger Foundation. I am grateful to the Perimeter Institute for hospitality, Niayesh Afshordi, Viqar Husain, Jose Lemos and Carlo Rovelli for stimulating discussions, and Swayamsiddha Maharana and Rama Vadapalli for helpful comments.

Appendix A: Equations and solutions

1. EMT structure and the Einstein equations

The effective EMT components of $k = 0$ Φ BHs outside the Schwarzschild radius r_g has the form

$$\tau_t = -\Upsilon^2 + e_{12}(t)\sqrt{x} + e_1(t)x + \mathcal{O}(x^{3/2}), \quad (A1)$$

$$\tau_t^r = -\Upsilon^2 + \phi_{12}(t)\sqrt{x} + \phi_1(t)x + \mathcal{O}(x^{3/2}), \quad (A2)$$

$$\tau^r = -\Upsilon^2 + p_{12}(t)\sqrt{x} + p_1(t)x + \mathcal{O}(x^{3/2}), \quad (A3)$$

where

$$\phi_{12} = \frac{1}{2}(e_{12} + p_{12}). \quad (A4)$$

The two subleading metric terms have the coefficients

$$c_1 = \left(\frac{1}{3} + \frac{4\sqrt{\pi}e_{12}r_g^{3/2}}{3\Upsilon} \right), \quad (A5)$$

$$h_{12} = \left(\frac{1}{3\sqrt{\pi}r_g^{3/2}\Upsilon} - \frac{e_{12} - 3p_{12}}{6\Upsilon^2} \right). \quad (A6)$$

We obtain higher order expressions by comparing expansions of the Einstein equations (8)–(10). We also quote the coefficient ℓ_1 of Eq. (21),

$$\ell_1 = -\sqrt{\xi} [c_{32}r_g - (1 - c_1)h_{12}r_g + 2\sqrt{\pi}r_g \Upsilon (2 - (2h_1 + h_{12}^2)r_g)] \quad (A7)$$

In the (v, r) coordinates convenient EMT components are obtained from $\Theta_{\mu\nu}$ as

$$\theta_v = e^{-2h_+} \Theta_{vv}, \quad \theta_{vr} = e^{-h_+} \Theta_{vr}, \quad \theta_r = \Theta_{rr}. \quad (A8)$$

Using the coordinate transformation Eq. (5) one can find relations between the effective EMT components in (v, r) with those in (t, r) ,

$$\theta_v = \tau_t, \quad \theta_{vr} = \frac{\tau_t^r - \tau_t}{f}, \quad \theta_r = \frac{\tau_t + \tau^r - 2\tau_t^r}{f^2}. \quad (A9)$$

The Einstein equations then take the following form

$$\partial_v C_+ = 8\pi r^2(\theta_v + f\theta_{vr}) \equiv 8\pi r^2\Theta_v^v, \quad (\text{A10})$$

$$\partial_r C_+ = -8\pi r^2\theta_{vr} \equiv -8\pi r^2\Theta_v^r, \quad (\text{A11})$$

$$\partial_r h_+ = 4\pi r\theta_r \equiv 4\pi r e^{h_+}\Theta_r^v. \quad (\text{A12})$$

Hence for solutions with $h_+ \equiv 0$ the relation $\tau_t + \tau^r = 2\tau_t^r$ holds identically.

2. Expansion coefficients and gap functions

Expanding the LHS of Eq. (A11) in a series around r_+ and the RHS around r_g , after making use of Eq. (A9), and comparing order-by-order, one arrives at the following relation for $w_1(v)$:

$$w_1(v) = \frac{e_{12} - p_{12}}{\Upsilon} \sqrt{\pi} r_g^{3/2} \quad (\text{A13})$$

The condition $e_{12}(t) = p_{12}(t)$ is therefore equivalent to $w_1(v) = 0$. Using Eqs. (23),(A5) and (A6) we can rewrite the redshift as

$$\alpha^2 = \frac{4\xi}{r_g}(1 - w_1). \quad (\text{A14})$$

Explicit leading order relations between different coordinates in the vicinity of the apparent horizon are based on Eq. (5). Starting from a point on the apparent horizon, $r_+(v) = r_g(t(v, r_+(v)))$, we relate the leading order coordinate differences $x = r - r_g(t)$ and $y = r - r_+(v)$.

First, consider the constant advanced coordinate. We thus evaluate the change in t from the value $t(v, r_+(v))$ along an ingoing null geodesic $v = \text{const.}$ Along such a geodesic the time $t(v, r)$ varies as

$$t(v, r_+ + y) = t(v, r_+) + \partial_r t|_{r_+} y + \frac{1}{2} \partial_r^2 t|_{r_+} y^2 + \mathcal{O}(y^3). \quad (\text{A15})$$

Determining the explicit form of the above relation requires evaluating partial derivatives at the apparent horizon. Eqs. (5) or (21) imply

$$\partial_r t = -e^{-h(t,r)} f(t, r)^{-1} = \frac{1}{r'_g} + \mathcal{O}(\sqrt{x}). \quad (\text{A16})$$

The time variation $\delta t := t(v, r_+ + y) - t(v, r_+)$ along an ingoing null geodesic is thus given by

$$\delta t = \frac{y}{r'_g} + \frac{1}{2} (\partial_r^2 t)|_{y=0} y^2 + \mathcal{O}(y^3). \quad (\text{A17})$$

The corresponding expansion of the Schwarzschild radius $r_g(t)$ is given by

$$r_g(t(v, r_+ + y)) = r_g(t(v, r_+)) + r'_g \delta t + \frac{1}{2} r''_g \delta t^2 + \mathcal{O}(\delta t^3), \quad (\text{A18})$$

where keeping terms of order δt^2 is crucial.

The coordinate distance $x(t, r) = r - r_g(t)$ is expressed as a function of the advanced null coordinate v and r ,

$$x(v, r_+ + y) = (r_+ + y) - r_g(t(v, r_+ + y)). \quad (\text{A19})$$

Using Eqs. (A17) and (A18) in (A19) along with the invariance of the MSH mass (6) then results in the quadratic relationship between x and y near the apparent horizon:

$$x = \frac{1}{2} \omega^2 y^2, \quad \text{where} \quad \omega^2 \equiv -r'_g (\partial_r^2 t)|_{y=0} - \frac{r''_g}{(r'_g)^2} \quad (\text{A20})$$

The second derivative of t over v is

$$\begin{aligned} \partial_v^2 t(v, r) &= \partial_v t \partial_t e^{-h+h_+} \\ &= \sqrt{\frac{x}{\xi}} e^{-2(\bar{h}-h_+)} \left(-\frac{r'_g}{2\sqrt{\xi}x} + \mathcal{O}(\sqrt{x}) \right), \end{aligned} \quad (\text{A21})$$

that at the apparent horizon becomes

$$\partial_v^2 t(v, r_+) = \frac{|r'_g|}{2\xi} \rightarrow \frac{1}{r_g}, \quad (\text{A22})$$

where the last expression on the RHS is valid when $w_1 = 0$ due to Eq. (29).

The second derivative of t over r is

$$\partial_r^2 t(v, r) = \frac{1}{(e^h f)^2} (\partial_r t \partial_t + \partial_r) e^h f \quad (\text{A23})$$

and using Eq. (21) we find

$$\partial_r^2 t(v, r_+) = -\frac{r''_g}{(r'_g)^2} - \frac{\ell_{12}^2}{2(r'_g)^3}. \quad (\text{A24})$$

This enables to give the explicit form to the parameter ω , as

$$\omega^2 = \frac{\ell_{12}^2}{2(r'_g)^2} \rightarrow \frac{1}{2\xi}, \quad (\text{A25})$$

when the last expression is again valid for $w_1 = 0$.

Then, using invariance of the MSH mass we observe

$$\begin{aligned} C_+(v, r) &= r_+(v) + w_1 y + \dots = C(t(v, r), r) \\ &= r_g(t(v, r_+)) + r'_g \left(\frac{y}{r'_g} \right) - 2\sqrt{2\pi r_g^3} \Upsilon \omega y + \dots \\ &= r_+ + \left(1 - 2\sqrt{2\pi r_g^3} \Upsilon \omega \right) y + \dots, \end{aligned} \quad (\text{A26})$$

and find

$$w_1 = 1 - 2\sqrt{2\pi r_g^3} \Upsilon \omega. \quad (\text{A27})$$

Now we obtain the leading term of the inverse transformation. For the constant time t integration of Eq. (5) leads to the

leading order expression

$$\delta v(x) = \frac{\sqrt{x}}{2\sqrt{\pi r_g \Upsilon}}. \quad (\text{A28})$$

Following the radius outwards at $t = \text{const}$ results in the relation $y(x)$,

$$y(t, r_g + x) = r_g + x - r_+(v + \delta v) = \frac{|r'_+| \sqrt{x}}{2\sqrt{\pi r_g \Upsilon}} + \mathcal{O}(x). \quad (\text{A29})$$

Expanding $C_+(v(t, r), r) = C(t, r)$ results in the identities such as $r'_+(1 - w_1) = -8\pi r_+^2 \Upsilon^2$ that follow from the transformation law of Eq. (A9) and the Einstein equation (A10).

3. Limits

The approximation of e^h via Eq. (38)

$$e^h \approx \sqrt{b^2 + \frac{\xi}{x}} + d, \quad (\text{A30})$$

allows to match the expansion of Eq. (34) up to h_{12} term for all finite values of r'_g (and, therefore, ξ and Υ).

The results of Section II B set the constraint

$$\frac{|r'_g|}{|r'_+|} = \frac{(1 - w_1)\sqrt{\xi}}{2\sqrt{\pi r_g^3 \Upsilon}}. \quad (\text{A31})$$

$$y_{\text{sep}} = \frac{2r_+(1 - w_1)r'_+}{1 + 2w_1^2 + (1 + 2r_+(w_2 - \chi_1))r'_+ - 2(1 + (1 - 2\chi_1 r_+)r'_+)w_1 - 2r_+w_1^2}. \quad (\text{B1})$$

Keeping only the leading order terms in $|r'_+| \ll 1$ and $w_1 \approx 0$ we obtain Eq. (57).

Appendix C: Painlevé–Gullstrand coordinates

Among the families of coordinates that are regular across the horizon [51, 53, 57] there are two types of the PG coordinates (\bar{t}, r) , where

$$\bar{t} = t + F(t, r) \quad (\text{C1})$$

is either the proper time of an infalling observer (with zero initial velocity at infinity) as the time coordinate, or chosen in such a way that the slices of constant \bar{t} have zero curvature. The two definitions are in general inequivalent, and it is the latter that is used in dynamical generalisations of the surface gravity. The flat slice condition leads the first-order linear par-

Assuming $w_1 = 0$, Page's evaporation law and the static limit, $c_1 \rightarrow w_1$, we find using the explicit expressions for c_1 , h_{12} and w_1 that

$$h_{12} \simeq \frac{1}{4\sqrt{\pi r_g^3 \Upsilon}}, \quad (\text{A32})$$

and thus

$$d = \sqrt{\xi} h_{12} = \frac{1}{2}, \quad b = \frac{1}{4}. \quad (\text{A33})$$

Using this approximation for e^h and $f \approx \alpha_{12}\sqrt{x} + x/r_g$, we obtain for the incoming null ray

$$\frac{dt}{dr} = -\frac{1}{e^h f} \approx -\frac{2r_g}{(\sqrt{x} + \alpha_{12}r_g)(\sqrt{x} + \sqrt{x + 4\xi})}, \quad (\text{A34})$$

that can be integrated in the closed form. For $r'_g \rightarrow 0$ the propagation time from $x_{\text{in}} \sim x_*$ to x_f according to Bob changes from $\delta t \sim (x_{\text{in}} - x_f)/|r'_g|$ transitions to the logarithmic divergence $\Delta t \sim r_g \ln(x_{\text{in}}/x_f)$.

Appendix B: Separatrix

Expanding Eq. (56) in the first order in $y = r - r_+$ results in

tial differential equation

$$\partial_r F = \sqrt{\frac{C}{r}} \frac{e^{-h}}{f} (1 + \partial_t F) =: \mathcal{A} \partial_{\bar{t}} \bar{t}, \quad (\text{C2})$$

where the sign choice is determined by the agreement with the standard (ingoing) PG coordinates for the Schwarzschild black hole.

Subject to appropriate boundary conditions this equation has a unique solution. The metric in (\bar{t}, r) coordinates is then

$$ds^2 = -\frac{e^{2h}}{(\partial_{\bar{t}} \bar{t})^2} d\bar{t}^2 + 2\frac{e^h}{\partial_{\bar{t}} \bar{t}} \sqrt{\frac{C}{r}} d\bar{t} dr + dr^2 + r^2 d\Omega, \quad (\text{C3})$$

For definiteness we choose $r_0 > r_g(t)$ such that

$$\bar{t}(t, r_0) = t, \quad (\text{C4})$$

a the initial condition.

In a slowly evolving case (where the evolution scale is set

by $|r'_g| \ll 1$ the PG is obtained iteratively. We set

$$\bar{t} = t + F_0(t, r) + F_1(t, r), \quad (\text{C5})$$

where F_0 satisfies $\partial_r F_0 = \mathcal{A}$ and thus

$$F_0 = F = \int_{r_0}^r \mathcal{A}(t, \tilde{r}) d\tilde{r}. \quad (\text{C6})$$

Then, instead of looking for the exact characteristic curves of the equation, we use the slow evolution condition to approximate

$$F_1 \approx \int_{r_0}^r \mathcal{A}(t, \tilde{r}) \partial_t F_0(t, \tilde{r}) d\tilde{r}. \quad (\text{C7})$$

Using the near-horizon metric of Eqs. (15) and (16), as well as expressions for the expansion coefficients in Appendix A 2 we get

$$\mathcal{A} = a_0 + a_{12} \sqrt{\frac{x}{\xi}} + \mathcal{O}(x), \quad (\text{C8})$$

where $a_0 = 1/|r'_g|$, and

$$a_{12} = -\frac{2(1-w_1)}{8\pi r_g^2 \Upsilon^2} - \frac{1}{2}. \quad (\text{C9})$$

It is further simplified if we assume $w_1 = 0$ and then Page's

evaporation law that results in Eq. (29). Hence,

$$a_{12} = \frac{1}{2} \left(1 - \frac{\alpha^2}{r_g'^2} \right) \approx -\frac{1}{|r_g'|}. \quad (\text{C10})$$

Hence

$$F_0 = \frac{x - x_0}{|r'_g|} + \frac{2a_{12}}{3\sqrt{\xi}} (x^{3/2} - x_0^{3/2}) + \mathcal{O}(x^2), \quad (\text{C11})$$

where $x_0 = r_0 - r_g$. Note that the magnitude of the second term is smaller than that of the first only if $x_0 \lesssim \xi$, and it dominates for $x \gg \xi$. It is straightforward to obtain the leading contribution to F_1 , but its expression is rather cumbersome. For our goal ($\partial \bar{t}(t, r)/\partial t$ on the apparent horizon) we can retain only the first term in F_0 . Then

$$F_1 \approx -\frac{(r_0 - r)^2 r_g''}{2(r_g')^3}, \quad (\text{C12})$$

and thus near the apparent horizon $F_1/F_0 = (r_0 - r)/r_g$. As a result the near-horizon form of the frozen metric in the PG coordinates is

$$\bar{t} = t + (r - r_0)/r_g + \mathcal{O}(x^{3/2}). \quad (\text{C13})$$

-
- [1] LIGO Scientific Collaboration, Virgo Collaboration, and KAGRA Collaboration, *Phys. Rev. X* **13**, 041039 (2023).
- [2] Event Horizon Telescope Collaboration, *Astrophys. J. Lett.* **930**, L16 (2022).
- [3] V. Cardoso and P. Pani, *Living Rev. Relativ.* **22**, 4 (2019).
- [4] E. Berti, V. Cardoso, G. Carullo, (eds.), arXiv:2505.23895 (2025).
- [5] S. W. Hawking and G. F. R. Ellis, *The Large Scale Structure of Space-Time* (Cambridge University Press, Cambridge, England, 1973).
- [6] V. P. Frolov and I. D. Novikov, *Black Hole Physics: Basic Concepts and New Developments* (Kluwer, Dordrecht, 1998).
- [7] V. Faraoni, *Cosmological and Black Hole Apparent Horizons* (Springer, Heidelberg, 2015).
- [8] M. Visser, *Phys. Rev. D* **90**, 127502 (2014).
- [9] C. Bambi, *Black Holes: A Laboratory for Testing Strong Gravity* (Springer Nature, Singapore, 2017).
- [10] R. B. Mann, S. Murk, and D. R. Terno, *Int. J. Mod. Phys. D* **31**, 2230015 (2022).
- [11] N. D. Birrel and P. C. W. Davies, *Quantum Fields in Curved Space* (Cambridge University Press, Cambridge, 1984).
- [12] R. Brout, S. Massar, R. Parentani, and P. Spindel, *Phys. Rep.* **260**, 329 (1995).
- [13] V. P. Frolov, arXiv:1411.6981 (2014).
- [14] L. Rezzolla and O. Zanotti, *Relativistic Hydrodynamics* (Oxford University Press, Oxford, England, 2013).
- [15] S. Murk, *Int. J. Mod. Phys. D* **32**, 2342012 (2023).
- [16] H. A. Buchdahl, *Phys. Rev.* **116**, 1027 (1959).
- [17] I. Soranidia and D. R. Terno, arXiv:2505.09189 (2025).
- [18] E. Franzin, S. Liberati and V. Vellucci, *JCAP* **2024**, 020 (2024).
- [19] P. K. Dahal, S. Maharana, F. Simovic, I. Soranidis, and D. R. Terno, *Phys. Rev. D* **110**, 044032 (2024).
- [20] É. É. Flanagan and R. M. Wald, *Phys. Rev. D* **54**, 6233 (1996).
- [21] C. Kiefer, *Quantum Gravity* (Oxford University Press, 2007).
- [22] B.-L. Hu and E. Verdaguer, *Semiclassical and Stochastic Gravity: Quantum Field Effects on Curved Spacetime* (Cambridge University Press, Cambridge, England, 2020).
- [23] P. K. Dahal, F. Simovic, I. Soranidis and D. R. Terno, *Phys. Rev. D* **108**, 104014 (2023).
- [24] V. Faraoni, G. F. R. Ellis, J. T. Firouzjaee, A. Helou, and I. Musco, *Phys. Rev. D* **95**, 024008 (2017).
- [25] S. Maharana and R. Vadapalli, arXiv:2509.11578 (2025).
- [26] E.-A. Kontou and K. Sanders, *Class. Quantum Gravity* **37**, 193001 (2020).
- [27] P. K. Dahal, I. Soranidis, and D. R. Terno, *Phys. Rev. D* **106**, 124048 (2022).
- [28] S. Maharana, F. Simovic, I. Soranidia, and D. R. Terno, *Phys. Rev. D* **111**, 104063 (2025).
- [29] D. Page, *New J. Phys.* **7**, 203 (2005).
- [30] J. M. Bardeen, *Phys. Rev. Lett.* **46**, 382 (1981).
- [31] LISA consortium, *Living Rev. Relativ.* **25**, 4 (2022).
- [32] B. Carr and J. Silk, *MNRAS* **478**, 3756 (2018).
- [33] C.-M. Yoo, *Galaxies* **10**, 112 (2022).
- [34] J. Auffinger, *Prog. Part. Nucl. Phys.* **131** 104040 (2023).
- [35] A. Ireland, S. Profumo and J. Scharnhorst *Phys. Rev. D* **107**, 104021 (2023).
- [36] K. S. Thorne, R. Price, and D. MacDonald (eds.), *Black Holes: The Membrane Paradigm* (Yale University, New Haven, CT,

- 1986).
- [37] E. Poisson, *A Relativist's Toolkit: The Mathematics of Black-Hole Mechanics* (Cambridge University Press, Cambridge, England, 2004).
- [38] A. Abedi, N. Afshordi, N Oshita, and Q Wang, *Universe* **6**, 43 (2020).
- [39] E. Maggio, L. Buoninfante, A. Mazumdar, and P. Pani, *Phys. Rev. D* **102**, 064053 (2020).
- [40] S. Chakraborty, E. Maggio, A. Mazumdar, and P. Pani, *Phys. Rev. D* **106**, 024041 (2022).
- [41] M. Silvestrini, E. Maggio, S. Chakraborty, and P. Pani, arXiv:2506.16516 (2025).
- [42] R. B. Mann, I. Nagle, and D. R. Terno, *Nucl. Phys. B* **936**, 19 (2018).
- [43] T. Jacobson, *Phys. Rev. Lett.* **75**, 1260 (1995).
- [44] T. Padmanabhan, *Class. Quantum Grav.* **19** 53879 (2002)
- [45] T. Padmanabhan, *Rep. Prog. Phys.* **73**, 046901 (2010).
- [46] P. K. Dahal and F. Simovic, arXiv:2304.11833 (2023).
- [47] J. W. York, Jr., *Phys. Rev. D* **28**, 2929 (1983).
- [48] V. P. Frolov, *Phys. Rev. D* **94**, 104056 (2016).
- [49] P. Binétruy, A. Helou, and F. Lamy, *Phys. Rev. D* **98**, 064058 (2018).
- [50] A. Ashtekar and B. Krishnan, *Living Rev. Relativ.* **7**, 10 (2004).
- [51] L. Vanzo, G. Acquaviva, and R. Di Criscienzo, *Class. Quantum Gravity* **28**, 183001 (2011).
- [52] B. Cropp, S. Liberati, and M. Visser, *Class. Quantum Gravity* **30**, 125001 (2013).
- [53] A. B. Nielsen and M. Visser, *Class. Quantum Gravity* **23**, 4637 (2006).
- [54] H. Kodama, *Prog. Theor. Phys.* **63**, 1217 (1980).
- [55] S. A. Hayward, *Class. Quantum Gravity* **15**, 3147 (1998).
- [56] R. B. Mann, S. Murk, and D. R. Terno, *Phys. Rev. D* **105**, 124032 (2022).
- [57] K. Martel and E. Poisson, *Am. J. Phys.* **69**, 476 (2001).
- [58] L. Rezzolla and A. Zhidenko, *Phys. Rev. D* **90**, 084009 (2014).
- [59] R. Konoplya, L. Rezzolla, and A. Zhidenko, *Phys. Rev. D* **93**, 064015 (2016).
- [60] R. A. Konoplya and A. Zhidenko, *Phys. Rev. D* **105**, 104032 (2022).